

# Interpreting Grokked Transformers in Complex Modular Arithmetic

Hiroki Furuta<sup>1</sup> Gouki Minegishi<sup>1</sup> Yusuke Iwasawa<sup>1</sup> Yutaka Matsuo<sup>1</sup>

## Abstract

Grokking has been actively explored to reveal the mystery of delayed generalization. Identifying interpretable algorithms inside the grokked models is a suggestive hint to understanding its mechanism. In this work, beyond the simplest and well-studied modular addition, we observe the internal circuits learned through grokking in complex modular arithmetic via interpretable reverse engineering, which highlights the significant difference in their dynamics: subtraction poses a strong asymmetry on Transformer; multiplication requires cosine-biased components at all the frequencies in a Fourier domain; polynomials often result in the superposition of the patterns from elementary arithmetic, but clear patterns do not emerge in challenging cases; grokking can easily occur even in higher-degree formulas with basic symmetric and alternating expressions. We also introduce the novel progress measure for modular arithmetic; *Fourier Frequency Sparsity* and *Fourier Coefficient Ratio*, which not only indicate the late generalization but also characterize distinctive internal representations of grokked models per modular operation. Our empirical analysis emphasizes the importance of holistic evaluation among various combinations.

## 1. Introduction

Grokking is a late generalization phenomenon when training Transformer (Vaswani et al., 2017) with algorithmic data (Power et al., 2022) where training accuracy soon reaches 100% with low test accuracy (often 0%), and after several iterations, test accuracy gradually reaches 100%. While grokking has been actively explored to reveal the mystery of delayed generalization, the interpretability analysis has mainly shed light on modular addition. With such simple synthetic data, grokking obtains the calculation with Fourier basis and trigonometric identities (Nanda et al., 2023; Zhong

<sup>1</sup>The University of Tokyo, Tokyo, Japan. Correspondence to: Hiroki Furuta <furuta@weblab.t.u-tokyo.ac.jp>.

et al., 2023; Gromov, 2023; Rubin et al., 2023). Identifying interpretable algorithms inside the grokked models should be a suggestive hint to understand grokking mechanism and dynamics. However, the mechanistic difference between the simplest and well-studied modular addition and other modular arithmetic, such as subtraction, multiplication, and polynomials, is still unclear. These analysis gaps would be problematic because we may not gain insight into real-world tasks with more complex data structures.

In this work, beyond the simplest and well-studied operation, we observe the internal circuits learned through grokking in complex modular arithmetic via interpretable reverse engineering<sup>1</sup>. In contrast to modular addition, the analysis across entire modular arithmetic would be challenging, since not all the operations have analytical algorithms. To mitigate such interpretability issues, we employ discrete Fourier transform and pre-grokked models, which have already grokked in the same or similar modular operations, as analysis tools. The results highlight the significant difference in grokking dynamics across entire modular arithmetic; subtraction poses a strong asymmetry on Transformer, and multiplication requires cosine-biased components at all the frequencies. Surprisingly, despite their difference, those elementary operations could find coexisting solutions when trained with a mixture. The learnable polynomials often result in the superposition of the patterns from elementary arithmetic, but clear patterns do not emerge in non-grokked operations. Grokking can easily occur in the sum of powers or even in higher-degree expressions factorizable with basic symmetric and alternating expressions. Furthermore, pre-grokked models with elementary arithmetic or a mixture of multi-operation could accelerate grokking in some simple cases.

Lastly, motivated by our empirical observations, we newly introduce the progress measure of grokking for modular arithmetic; *Fourier Frequency Sparsity* (FFS) and *Fourier Coefficient Ratio* (FCR), which not only indicate the late generalization but also characterize distinctive representations inside the grokked models for each operation. We prove that our proposed FFS and FCR decrease accompanying the test accuracy improvement, and they reflect features of internal circuits, such as the coexistence of addition and

<sup>1</sup>[https://github.com/frm03/grok\\_mod\\_poly](https://github.com/frm03/grok_mod_poly)

	Elementary	Linear	PG-E→Linear	Cross ( $n = 1$ )	PG-T→Cross ( $n = 1$ )	Univariate	Cross ( $n \geq 2$ )	Powers	Factorizable
Grok?	✓	$r = 0.4$	✓	$r = 0.5$	✓	✓	✗	✓	✓

Table 1. Summary of grokked modular operators ( $p = 97$ ) – if they occur grokking in  $r = 0.3$  or not. We provide the smallest train fraction where grokking happens. PG-E/T stands for pre-grokked embedding/Transformer. See Appendix I for more detailed results.

multiplication patterns in  $ab + b$ , or dependence of the factorizable polynomials on the parity of exponent  $n$ . Our empirical analysis emphasizes and the importance of holistic investigation among synthesized datasets with various rules. In summary, our key observations are:

- In elementary arithmetic, modular addition, subtraction, and multiplication learn distinct representations in the Fourier domain, while allowing coexistence in multi-task training.
- In polynomials, grokked models often exhibit a superposition of representations in elementary arithmetic.
- The sum of powers and polynomials factorizable with linear addition (subtraction) easily induce grokking, even in the case of higher degrees (e.g.  $n = 7$ ). In contrast, ones with the cross term ( $n \geq 2$ ) are hard to grok (Table 1).
- Pre-grokked models and a mixture of multi-operation accelerate grokking among similar operations.
- The decrease of either FFS or FCR (or both) indicates the progress of grokking, and they also characterize each representation of modular operations.

## 2. Related Work

**Grokking** Grokking has been actively studied to answer the questions: (1) when it happens, (2) why it happens, and (3) what representations are learned. In simple algorithmic tasks like modular addition, grokking would be observed with proper weight decay and the ratio of train-test splits (Power et al., 2022; Lyu et al., 2023). In addition to synthetic data (Liu et al., 2023b), grokking could occur in more general settings such as teacher-student (Levi et al., 2023), NLP (Murty et al., 2023), computer vision (Thilak et al., 2022), or molecular graph tasks (Liu et al., 2023a) due to the mismatch between the train-test loss landscape against weight norm (Liu et al., 2023a). Recent findings have revealed that while grokking has initially been observed in neural networks (MLP and Transformer), it also occurs in Gaussian processes and linear regression models (Kumar et al., 2023; Levi et al., 2023; Rubin et al., 2023; Miller et al., 2023). Our work focuses on complex modular arithmetic including subtraction, multiplication, polynomials, and a multi-task mixture, and then discusses the difference between grokked and non-grokked modular operations.

Several works have argued that the late generalization dynamics has been driven by the sparsification of neural network emerging dominant sub-networks (Merrill et al., 2023;

Tan & Huang, 2023) and the structured representations (Liu et al., 2022); the training process could be a phase transition divided into memorization, circuit formation, and cleanup phase (Nanda et al., 2023; Xu et al., 2023; Doshi et al., 2023; Davies et al., 2023; Žunkovič & Ilievski, 2022), and the formation of generalization circuits produces higher logits with small norm parameters than memorization circuits (Varma et al., 2023). The sparse lottery tickets in neural networks may also promote grokking (Minegishi et al., 2023). Moreover, our work highlights that in modular arithmetic such sparse representations are obtained interpretably through the discrete Fourier transform.

**Mechanistic Interpretability** While training neural networks is often accompanied by mysterious phenomena such as double descent (Nakkiran et al., 2019), many works along the mechanistic interpretability have attempted to systematically understand what happened during training and inference through extensive reverse engineering (Olah et al., 2020; Olsson et al., 2022; Akyürek et al., 2023; Elhage et al., 2022; Notsawo et al., 2023). Paying attention to the activation of neurons, those studies have tried to identify the functional modules or circuits inside neural networks (Elhage et al., 2021; Conmy et al., 2023). Even for recent large language models, controlling activation patterns via activation patching can unveil the role of each module (Vig et al., 2020; Meng et al., 2023; Zhang & Nanda, 2024). In grokking literature, several works have revealed what kind of algorithmic pattern was obtained inside the model when it worked on modular addition (Zhong et al., 2023; Nanda et al., 2023; Morwani et al., 2023) or group composition (Chughtai et al., 2023; Stander et al., 2023) through the Fourier transform of logits or investigating gradients. Gromov (2023) points out that the learned weights and algorithms in some arithmetic tasks are analytically solvable if MLP uses a quadratic activation. In contrast, we provide a detailed analysis of entire modular arithmetic, while extending the range of operations from addition to subtraction, multiplication, and polynomials, as well as a multi-task mixture, which do not always have analytical algorithms.

## 3. Preliminaries

**Grokking** This paper focuses on grokking on the classification tasks from simple algorithmic data commonly investigated in the literature (Power et al., 2022; Liu et al., 2022; Barak et al., 2022). We have train and test datasets ( $S_{\text{train}}$ ,  $S_{\text{test}}$ ) without overlap, and learn a neural network  $f(\mathbf{x}; \boldsymbol{\theta})$  where  $\mathbf{x}$  is an input vector and  $\boldsymbol{\theta}$  are weights of neural

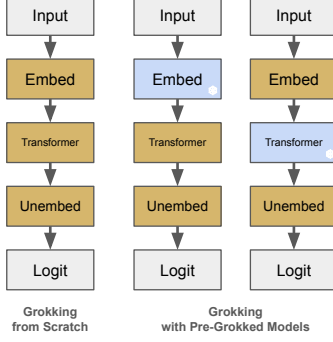


Figure 1. Grokking has been investigated with training from scratch. To shed light on the dynamics inside Transformer, we introduce the notion of *pre-grokked models*, which are pre-trained on a similar task until grokking and used to replace randomly initialized modules without any parameter updates (i.e. frozen). We use pre-grokked embedding and Transformer in the later section.

network. The small-size Transformers (e.g. one or two layers) or MLP are usually employed as an architecture of  $f$ . Specifically, they train the network using stochastic gradient decent over the cross-entropy loss  $\mathcal{L}$  and weight decay:

$$\theta \leftarrow \operatorname{argmin}_{\theta} \mathbb{E}_{(x,y) \sim S} \left[ \mathcal{L}(f(x; \theta), y) + \frac{\lambda}{2} \|\theta\|_2 \right],$$

where  $y \in \{0, \dots, p-1\}$  is a scalar class label correspond to the inputs  $x$ , and  $\lambda$  is a hyper-parameter controlling the regularization. Note that weight decay is critical for the grokking phenomenon (Power et al., 2022; Liu et al., 2023a), and we employ AdamW (Loshchilov & Hutter, 2019)) as an optimizer in practice. The fraction of training data from all the combinations is defined as:

$$r = \frac{|S_{\text{train}}|}{|S_{\text{train}}| + |S_{\text{test}}|} \left( = \frac{|S_{\text{train}}|}{p^2} \right).$$

It has been observed that a larger fraction tends to facilitate fast model grokking, whereas a smaller fraction makes grokking more challenging and slow especially in complex settings such as modular polynomial tasks.

**Transformers** As discussed in Elhage et al. (2021), the functionality of a small-scale Transformer can be written down with several distinctive matrices. We denote embedding weights as  $W_E \in \mathbb{R}^{d_{\text{emb}} \times p}$ , output weights at the last MLP block as  $W_{\text{out}} \in \mathbb{R}^{d_{\text{emb}} \times d_{\text{mlp}}}$ , and unembedding weights as  $W_U \in \mathbb{R}^{p \times d_{\text{emb}}}$ . The logit vector on inputs  $a, b$  can be approximately written with activations from MLP block,  $\text{MLP}(a, b)$ , as  $\text{Logits}(a, b) \approx W_U W_{\text{out}} \text{MLP}(a, b)$  by ignoring residual connection (Nanda et al., 2023), and we investigate the neuron-logit map  $W_L = W_U W_{\text{out}} \in \mathbb{R}^{p \times d_{\text{mlp}}}$  in the later analysis. See Appendix C for further details.

**Analysis in Modular Addition** Nanda et al. (2023) have first pointed out that Transformer uses particular Fourier components and trigonometric identities after grokking occurred in modular addition. The modular addition is a basic

mathematical operation as  $(a + b) \% p = c$  where  $a, b, c$  are integers. The model predicts  $c$  given a pair of  $a$  and  $b$ . As a slightly abused notation,  $a, b, c$  may represent one-hot representation, and we will omit  $\% p$  in later sections.

In the case of modular addition, the way Transformer model represents the task has been well-studied (Zhong et al., 2023; Nanda et al., 2023), where the embedding matrix  $W_E$  maps the input one-hot vectors into cosine and sine functions for various frequencies  $\omega_k = \frac{2k\pi}{p}$ ,  $k \in \{0, \dots, p-1\}$ ,

$$a \rightarrow \cos(\omega_k a), \sin(\omega_k a).$$

It is also known that the addition is implemented inside the Transformer with trigonometric identities,

$$\begin{aligned} \cos(\omega_k(a + b)) &= \cos(\omega_k a) \cos(\omega_k b) - \sin(\omega_k a) \sin(\omega_k b), \\ \sin(\omega_k(a + b)) &= \sin(\omega_k a) \cos(\omega_k b) + \cos(\omega_k a) \sin(\omega_k b), \end{aligned}$$

and then the neuron-logit map  $W_L$  reads off  $\cos(\omega_k(a + b - c))$  by also using trigonometric identities,

$$\begin{aligned} \cos(\omega_k(a + b - c)) &= \\ &\cos(\omega_k(a + b)) \cos(\omega_k c) + \sin(\omega_k(a + b)) \sin(\omega_k c). \end{aligned} \tag{1}$$

The logits of  $c$  are the weighted sum of  $\cos(\omega_k(a + b - c))$  over  $k$ . Note that we only consider the first half of frequencies (i.e.  $k \in \{1, \dots, \lfloor \frac{p}{2} \rfloor\}$ ) because of the symmetry.

### 3.1. Experimental Setup

In this paper, we expand the discussion above on modular addition to entire modular arithmetic:  $a \circ b \% p = c$  where  $\circ$  represents arbitrary operations (or polynomials) that take two integers  $a$  and  $b$  as inputs, such as  $a - b$  (subtract),  $a * b$  (multiplication),  $2a - b$ ,  $ab + b$ ,  $a^2 + b^2$ ,  $a^3 + ab$ ,  $(a + b)^4$  (polynomials)<sup>2</sup>. Transformer takes three one-hot tokens as inputs,  $a, \circ, b$ . In addition to  $p$  integer tokens, we prepare  $n_{\text{op}}$  special tokens representing the mathematical operations above. The models are trained to predict  $c$  as an output.

Our neural network is composed of a single-layer Transformer architecture (Figure 1) with learnable embedding and unembedding ( $d_{\text{emb}} = 128$ ). We use ReLU for the activation functions and remove positional embedding, layer normalization, and bias terms for all the layers. This Transformer is trained via full batch gradient descent with AdamW (Loshchilov & Hutter, 2019) and weight decay  $\lambda = 1.0$ . We use  $p = 97$  for all the experiments. For the dataset fraction, we use  $r = 0.3$  unless otherwise mentioned. Other hyper-parameters are described in Appendix A.

<sup>2</sup>We omit the discussion on modular division, since it requires division into cases while we also consider a multi-task mixture.

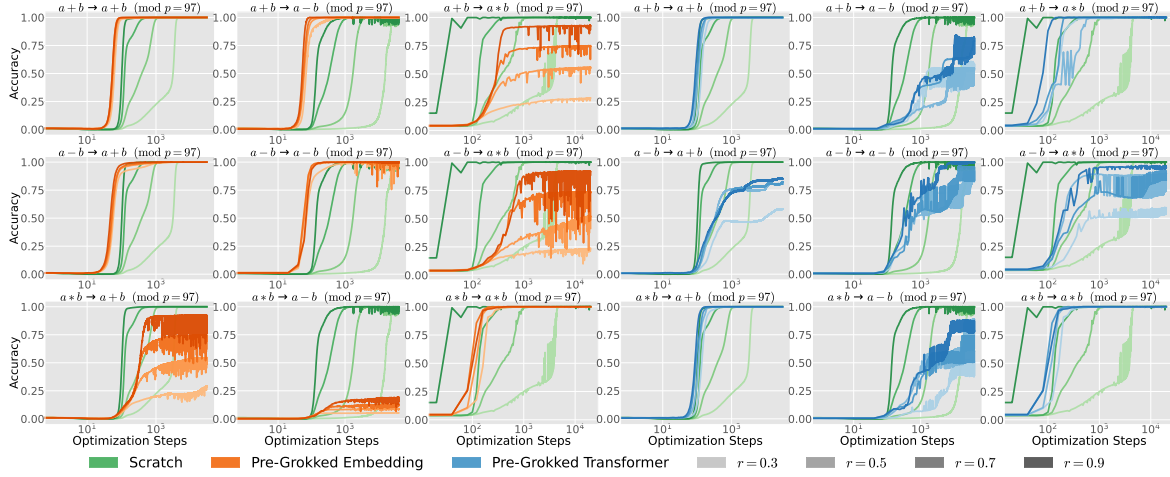


Figure 2. Test accuracy in modular elementary arithmetic (addition, subtraction, and multiplication) with pre-grokked models (embedding and Transformer). The x-axis is the logarithmic scale. Because of the task simplicity, grokking always occurs in elementary arithmetic. However, in certain combinations, pre-grokked models hinder grokking even with a  $r = 0.9$  fraction. For pre-grokked embedding, addition and subtraction accelerate grokking each other (fig[0:2, 0:2]), while multiplication and those do not show synergy (+: fig[2, 0] and [0, 2], -: fig[2, 1] and [1, 2]). In contrast, for pre-grokked Transformer, subtraction is challenging in both directions, even transferring subtraction models into subtraction itself (fig[1, 4]). Addition and multiplication accelerate each other (fig[0, 5] and [2, 3]).

#### 4. Pre-Grokked Models and Fourier Metrics

In contrast to modular addition, the analysis across entire modular arithmetic would be challenging, since not all the operations have analytical algorithms. To mitigate such interpretability issues, we introduce the notion of *pre-grokked models*, and propose a pair of novel progress measures for grokking in modular arithmetic: *Fourier Frequency Sparsity (FFS)* and *Fourier Coefficient Ratio (FCR)*, which are derived from our empirical observation on sparsity and sinusoidal bias in embedding and neuron-logit map layers.

**Pre-Grokked Models** To dive into the dynamics inside Transformer, we leverage pre-grokked models, which are pre-trained on similar algorithmic tasks until grokking and used for another training to replace randomly initialized modules without any parameter updates (i.e. frozen). This allows us to consider learning representations and algorithms separately. We will use pre-grokked embedding and pre-grokked Transformer in the later section.

**Fourier Frequency Sparsity (FFS)** FFS quantitatively measures the sparsity of Fourier components in a certain layer (embedding or neuron-logit map),

$$\text{FFS}(\eta, \mu, \nu) =$$

$$\frac{1}{2 \lceil \frac{p}{2} \rceil} \sum_k^{\lceil \frac{p}{2} \rceil} \mathbb{1} \left[ \frac{\|\mu_k\|_2}{\max_i \|\mu_i\|_2} > \eta \right] + \mathbb{1} \left[ \frac{\|\nu_k\|_2}{\max_j \|\nu_j\|_2} > \eta \right],$$

where  $u_k \in \mu = \{\mu_1, \dots, \mu_k, \dots\}$  is a coefficient of cosine components and  $\nu_k \in \nu$  is a coefficient of sine components with frequency  $\omega_k$ . We set  $\eta = 0.5$ . The low FFS indicates that a few key frequencies are dominant in the Fourier

domain, which can be often observed in modular addition.

**Fourier Coefficient Ratio (FCR)** FCR quantifies the sinusoidal bias of Fourier components in a certain layer,

$$\text{FCR}(\mu, \nu) = \frac{1}{\lceil \frac{p}{2} \rceil} \sum_k^{\lceil \frac{p}{2} \rceil} \min \left( \frac{\|\mu_k\|_2}{\|\nu_k\|_2}, \frac{\|\nu_k\|_2}{\|\mu_k\|_2} \right).$$

The low FCR means that Fourier representations of the weights have either cosine- or sine-biased components, which can be often observed in modular multiplication.

The decrease of either FFS or FCR (or both) indicates the progress of grokking, and the responsible indicator depends on each modular operation; for instance, FFS is a good measure for addition, and FCR is for multiplication. They are not only aligned with the late improvement in test accuracy but also can characterize each Fourier representation of modular operations at a certain layer.

#### 5. Analysis in Elementary Arithmetic

The analysis with pre-grokked models can reveal the characteristics of each arithmetic operation; if pre-grokked embedding encourages grokking in downstream tasks, the learned embedding should be similar, but if not, those tasks should require different types of representations. Moreover, if a pre-grokked Transformer accelerates generalization, it means the algorithms obtained internally would have similar properties, while the failure hints at the algorithmic difference.

Figure 2 shows test accuracy in elementary arithmetic (addition, subtraction, and multiplication) with pre-grokked

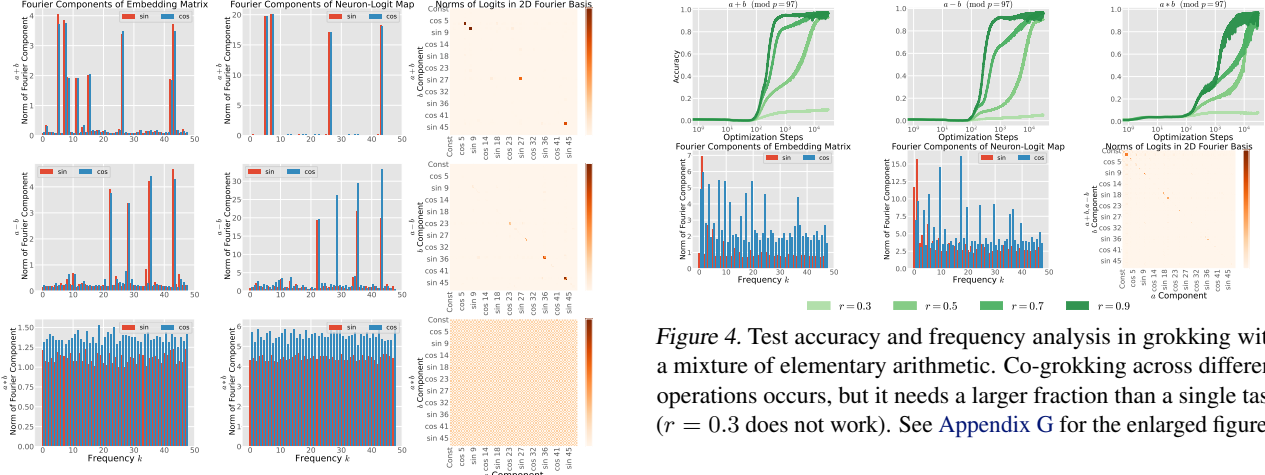


Figure 3. Frequency analysis in grokking with elementary arithmetic. Subtraction learns similar embedding to addition with sparse Fourier components (fig[0, 0] and fig[1, 0]). However, it imposes an asymmetric neuron-logit map and norm of logits with cosine biases (fig[1, 1] and fig[1, 2]). Multiplication obtains quite a different embedding from others (fig[2, :]); it employs all the frequencies equally with cosine bias for both embedding and neuron-logit map. See Appendix G for the enlarged version.

embedding and Transformer<sup>3</sup>. Because of the task simplicity, grokking always occurs among those operations. However, in certain combinations, pre-grokked models hinder grokking even with a  $r = 0.9$  fraction. For pre-grokked embedding, modular addition and subtraction accelerate grokking (Figure 2[0:2, 0:2]), while modular multiplication and those two hurt the performances each other (+: Figure 2[2, 0] and [0, 2], -: Figure 2[2, 1] and [1, 2]). In contrast, for pre-grokked Transformer, modular subtraction is challenging in both directions, even transferring subtraction models into subtraction itself (Figure 2[1, 4]). Pre-grokked Transformer on addition or multiplication accelerates each other (Figure 2[0, 5] and [2, 3]). Those results imply that (1) while there is a similarity between the learned embeddings in addition and subtraction, their acquired algorithms significantly differ (Section 5.1), and that (2) multiplication requires representations independent of addition or subtraction but the algorithm might be transferable (Section 5.2).

## 5.1. Modular Subtraction Imposes Strong Asymmetry

Considering the sign in trigonometric identities, Transformers should learn modular subtraction in the Fourier domain with trigonometric identities as the case of addition (Equation 1):

$$\begin{aligned} \cos(\omega_k(a - b - c)) = \\ \cos(\omega_k(a - b)) \cos(\omega_k c) + \sin(\omega_k(a - b)) \sin(\omega_k c), \end{aligned}$$

<sup>3</sup>To avoid the confusion, we will mention the sub-figures using pythonic coordinates like Figure[i, j] for row i column j.

Figure 4. Test accuracy and frequency analysis in grokking with a mixture of elementary arithmetic. Co-grokking across different operations occurs, but it needs a larger fraction than a single task ( $r = 0.3$  does not work). See Appendix G for the enlarged figure.

and then we would anticipate similar interpretable representations to addition. However, we observe that the grokked models exhibit asymmetric properties for both embedding and Transformer. We transform the embedding into a Fourier domain along the input dimension and compute the L2 norm along other dimensions. In Figure 3, subtraction learns similar embedding to addition with sparse Fourier components (Figure 3[0, 0] and [1, 0]). On the other hand, it imposes an asymmetric neuron-logit map and norms of logits with cosine-biased components (Figure 3[1, 1] and [1, 2]), which may represent alternatings ( $a - b \neq b - a$ ).

Such an asymmetry is also observed in grokked Transformers. As discussed in Figure 2, the pre-grokked Transformer on subtraction could not be transferred to **any** downstream elementary arithmetic (Figure 2[1, :]), even subtraction itself (Figure 2[1, 4]), and pre-grokked models with addition or multiplication could not learn subtraction as well (Figure 2[:, 4]). This implies that while we could interpret subtraction as a part of addition with negative numbers, the embedding and algorithm inside Transformer are quite different.

Lastly, we examine the restricted loss and ablated loss in Appendix E, where the restricted loss is calculated only with the Fourier components of significant frequencies, and the ablated loss is calculated by removing a certain frequency from the logits. The analysis emphasizes the subtle dependency on other frequencies than significant ones.

## 5.2. Modular Multiplication Leverages All Frequencies

In contrast to modular addition and subtraction, we may not describe possible acquired algorithms for modular multiplication in a closed form, since trigonometric identities do not have multiplication formulas. However, following the analysis in modular addition, we can observe that multiplication also leverages the periodicity in the Fourier domain.

Figure 3 reveals that multiplication obtains significantly different Fourier representation from addition or subtraction

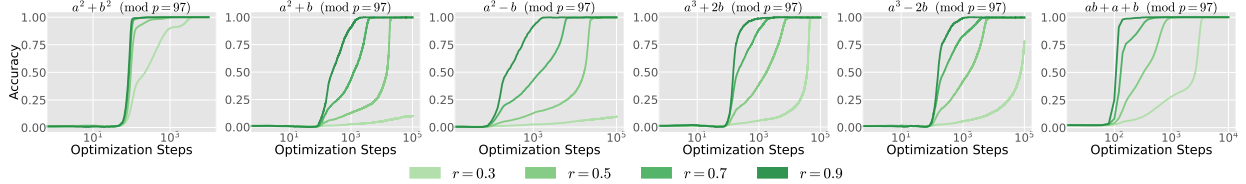


Figure 5. Test accuracy in modular polynomials (univariate terms:  $a^2 + b^2$ ,  $a^2 \pm b$ ,  $a^3 \pm 2b$ , the degree-1 with cross term:  $ab + a + b$ ). Grokking occurs even in quadratic or cubic expressions asymmetric with input  $a$  and  $b$ .

(Figure 3[2, :]); it employs all the frequencies equally with cosine bias for both embedding and neuron-logit map.

Surprisingly, multiplication-pre-grokked Transformer accelerates grokking in addition (Figure 2[2, 3]) and addition-pre-grokked Transformer (Figure 2[0, 5]) can cause grokking in multiplication. This implies that in contrast to the asymmetry of subtraction, addition and multiplication leverage their symmetry in the operations. Since the embedding of multiplication is quite different from addition and subtraction, it is reasonable to fail to grok with addition/subtraction-pre-grokked embeddings (Figure 2[0:2, 2] and [2, 0:2]). Moreover, we find that grokking in elementary arithmetic occurs even with frozen random embedding (see Appendix F) that does not have biased components nor sparsity, while the neuron-logit map obtains a similar representation as in Figure 3. This emphasizes some unique, non-transferable patterns are learned in grokked models.

### 5.3. Multi-Task Mixture Discovers Coexisting Solutions

To fill the gap between synthetic tasks and practice, we here investigate grokking on mixed datasets with addition, subtraction, and multiplication.

Figure 4 reveals that *co-grokked* (i.e. grokking happens for all the tasks) occurs, but it requires a larger fraction of train dataset than a single task; for instance,  $r = 0.3$  could not cause grokking while it does in Figure 2. The test accuracy of multiplication increases slower than the other two, which implies the conflict among different Fourier representations may affect the performance and generalization.

For the Fourier analysis of grokked models, training with a multi-task mixture seems to discover “Pareto-optimal” representations for all the operations in embedding and neuron-logit map (Figure 4[1, :]). We can see the coexistence of component sparsity in embedding (addition), asymmetric cosine sparsity in neuron-logit map (subtraction), and cosine-biased components for all the frequencies (multiplication). Furthermore, the norms of logits in 2D Fourier basis for addition and subtraction exhibit the same patterns. This means that addition and subtraction can be expressed on the same representation space originally, while they find quite different grokked models after the single-task training. It would be an interesting future direction to further reveal the

grokking dynamics and mechanism for multi-task training.

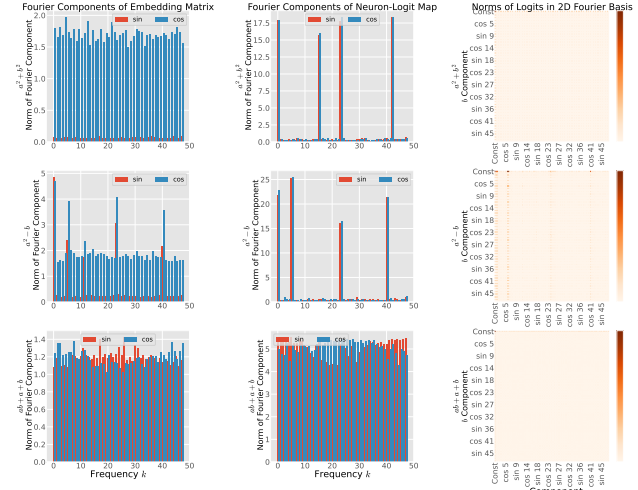


Figure 6. Frequency analysis in grokking with modular polynomials ( $a^2 + b^2$ ,  $a^2 - b$ ,  $ab + a + b$ ). Grokking discovers the superposition of frequency sparsity and bias seen in elementary arithmetic;  $a^2 - b$  inherits both biased sparsity in subtraction and significant cosine biases in multiplication for embedding (fig[1,0]). Its neuron-logit map leverages addition-like sparsity (fig[1,1]). See Appendix G for the enlarged version.

## 6. Analysis in Polynomials

It has been known that grokking would be less likely to occur as increasing the complexity of operators in general (Power et al., 2022), but the underlying reasons or conditions are still unclear. In addition to elementary operations, we examine the interpretable patterns of grokked models in modular polynomials. We first investigate the case of simple polynomials (Section 6.1), quadratic, cubic, and quartic expressions (Section 6.2) and linear expressions with pre-grokked models (Section 6.3). We also study multi-task training mixing hard and easy operations (Appendix D).

### 6.1. Polynomials Discover Superposition of Representations for Elementary Arithmetic

We here investigate the relatively simple polynomials that induce grokking (univariate terms:  $a^2 + b^2$ ,  $a^2 \pm b$ ,  $a^3 \pm 2b$ , the degree-1 with cross term:  $ab + a + b$ ). In Figure 5, grokking occurs even in quadratic or cubic expressions asymmetric

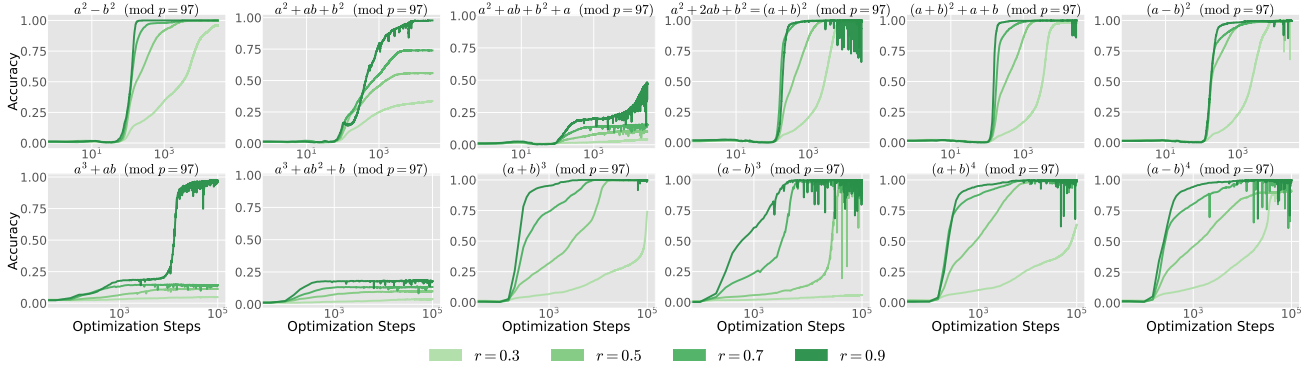


Figure 7. Test accuracy in modular polynomials with quadratic, cubic, and quartic formulas. Transformers suffer from late generalization in degree- $n$  polynomials with cross-term ( $a^2 + ab + b^2$ ,  $a^2 + ab + b^2 + a$ ,  $a^3 + ab$ ,  $a^3 + ab^2 + b$ ). If polynomials are factorizable with addition ( $a + b$ ) or subtraction ( $a - b$ ), they are easy to grok (e.g.  $(a + b)^2 + a + b$ ; fig[0][4]) although they also have a cross term (c.f.  $a^2 + ab + b^2$ ). Even, cubic ( $(a \pm b)^3$ ; fig[1][2:4]) or quartic ( $(a \pm b)^4$ ; fig[1][4:]) expressions, grokking occurs if they are factorizable.

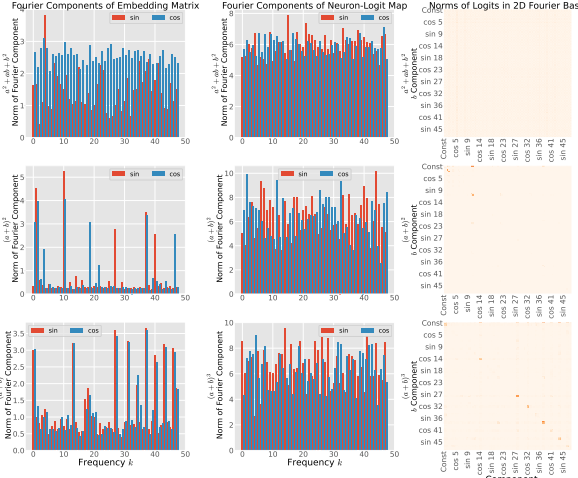


Figure 8. Frequency analysis in grokking with factorizable polynomials. Compared to non-factorizable one ( $a^2 + ab + b^2$ , fig[0, :]), which cannot find sparse embedding representations, factorization with elementary arithmetic accelerates grokking in both quadratic ( $(a + b)^2$ , fig[1, :]) and cubic expression ( $(a + b)^3$ , fig[2, :]) with sparse Fourier features. See Appendix G for the enlarged version.

with input  $a$  and  $b$ , and suggests that the existence of symmetry or the cross term might be a key for occurrence.

Moreover, the grokked models exhibit partially-similar internal states to the one in elementary arithmetic. Figure 6 provides frequency analysis with modular polynomials ( $a^2 + b^2$ ,  $a^2 - b$ ,  $ab + a + b$ ), where grokking discovers superposition of representations (frequency sparsity and bias) for elementary arithmetic. For instance,  $a^2 + b^2$  finds a cosine-biased embedding like multiplication and a sparse neuron-logit map like addition.  $a^2 - b$  inherits both biased sparsity in subtraction and significant cosine biases in multiplication for embedding. Its neuron-logit map leverages addition-like sparsity.  $ab + a + b$  is similar to multiplication; leveraging biased all the frequencies while using sine components,

because it can be factorized as  $(a + 1)(b + 1) - 1$ . These trends are flipped between embedding and neuron-logit map. Norms of logits in 2D Fourier basis basically follow the trend in multiplication (Figure 6[:, 2]), and especially  $a^2 - b$  activates key frequency columns (Figure 6[1, 2]).

## 6.2. High-Degree Factorization Allows Grokking

Increasing the complexity of operators, we test modular polynomials with quadratic, cubic, and quartic formulas in Figure 7. Apparently, Transformer fails to generalize in degree- $n$  polynomials with cross term ( $a^2 + ab + b^2$ ,  $a^2 + ab + b^2 + a$ ,  $a^3 + ab$ ,  $a^3 + ab^2 + b$ ). However, if polynomials are factorizable with addition (subtraction) or are the sum of powers, they easily grok, although they also have cross terms (e.g.,  $(a + b)^2 + a + b$ ). Even, cubic (Figure 7[1, 2:4]) or quartic (Figure 7[1, 4:]) expressions, grokking occurs if they are factorizable. Comparing  $a^2 + ab + b^2$  and  $(a + b)^2$  or  $a^2 + ab + b^2 + a$  and  $(a + b)^2 + a + b$  emphasizes the importance of factorizability for the emergence of grokking.

Figure 8 analyzes the frequency components in factorizable polynomials. Compared to non-factorizable one ( $a^2 + ab + b^2$ ), which cannot find the sparse embedding representation, factorizable operations promote grokking in both quadratic ( $(a + b)^2$ ) and cubic expression ( $(a + b)^3$ ) obtaining sparsity in embedding. The factorizable polynomials exhibit clear logits patterns as shown in elementary arithmetic (Figure 3), while non-factorizable ones only show significant norms around a constant component.

## 6.3. Pre-Grokked Models Accelerate Grokking in Linear Expression

The experiments suggest that grokked models obtain meaningful embedding or circuits inside the Transformer. From

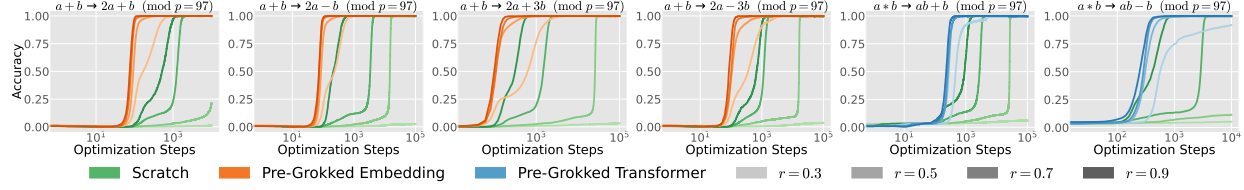


Figure 9. Test accuracy in modular linear expression ( $2a \pm b$ ,  $2a \pm 3b$ ) and degree-1 polynomials with cross term ( $ab \pm b$ ). Pre-grokked embedding in modular addition accelerates grokking in  $2a \pm b$ ,  $2a \pm 3b$ , and pre-grokked Transformer in modular multiplication accelerates grokking in  $ab \pm b$ , while the training from scratch could not generalize in  $r = 0.3$ .

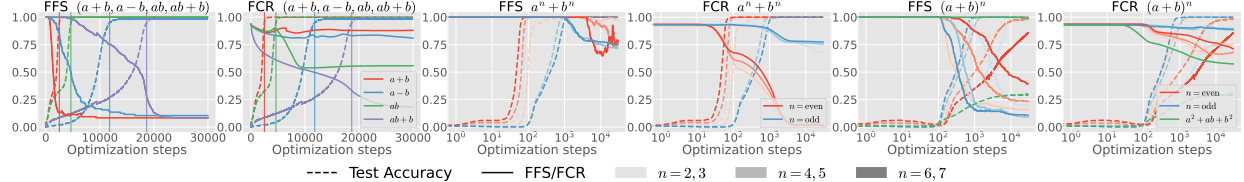


Figure 10. FFS and FCR as progress measure of grokking. The decrease of either FFS or FCR (or both) indicates the progress of grokking synchronizing with the test accuracy improvement. The responsible indicator depends on each operation. See Appendix H for the details.

another perspective, we can hypothesize that pre-grokked models in a certain task could promote grokking in other similar tasks, because they already have a useful basis.

We test whether frozen pre-grokked modules in elementary arithmetic ( $a + b$ ,  $a * b$ ) are transferable to grokking in modular linear expression ( $2a \pm b$ ,  $2a \pm 3b$ ,  $ab \pm b$ ). Those asymmetric expressions are hard to grok from scratch, especially if the fraction is small ( $r = 0.3$ ) despite their simplicity. Figure 9 shows that pre-grokked embedding with addition accelerates grokking in  $2a \pm b$ ,  $2a \pm 3b$ , and pre-grokked Transformer with multiplication does in  $ab \pm b$ . These support our hypothesis and imply that in complex operations, internal circuits struggle with finding interpretable patterns.

## 7. FFS and FCR as Progress Measures

As shown in Figure 10, we measure FFS and FCR in embedding layer  $W_E$  for various modular operations. See Appendix H for the results in neuron-logit map  $W_L$ .

**Elementary Arithmetic** Addition (red) and subtraction (blue) decrease FFS and keep a high FCR, whereas multiplication maintains FFS as 1.0 and decreases FCR (green). In all the cases, the saturation of accuracy and inflection point of either FFS or FCR almost match (vertical lines). Interestingly,  $ab + b$  (purple) exhibits decreasing both FFS and FCR, which reflects the feature of addition and multiplication simultaneously.

**Sum of Powers** In  $a^n + b^n$ , FFS and FCR exhibit the same progress as multiplication, while the neuron-logit map has sparsity the same as addition (Appendix H). We also observe the different behaviors depending on the parity of exponent  $n$ ; FFS decreases more when  $n$  is odd (blue), and FCR drops more when  $n$  is even (red).

**Factorizable Polynomials**  $(a + b)^n$  exhibits the same trend as addition: high sparsity and balanced components. In contrast, the neuron-logit map behaves similarly to multiplication (Appendix H). As in the sum of powers, the dynamics would be different depending on the parity of exponent  $n$ ; FCR significantly drops when  $n$  is even. In the case of non-factorizable  $a^2 + ab + b^2$ , FFS do not change during training, and the model cannot achieve late generalization.

## 8. Conclusion

Our analysis has shed light on significant differences in grokking dynamics across modular arithmetic. We have opposite observations to well-known analysis in modular addition; even among modular elementary arithmetic, they each learn distinct representations inside Transformer, featured by Fourier frequency sparsity and Fourier coefficient ratio; subtraction obtains sparse and asymmetric Fourier components, while multiplication leverages dense and cosine-biased ones. In polynomials, the grokked models have the superposition of Fourier representation in elementary arithmetic and the emergence of grokking is dependent on the operation’s signal-to-noise ratio; the factorizable polynomials with addition or subtraction are much easier to grok, and grokking can be accelerated with pre-grokked models or a mixture of modular arithmetic. To interpret grokking mechanistically, it is essential to holistically evaluate all the possible algorithmic data as possible.

**Limitation** We assume that all modular arithmetic can be solved with the Fourier basis and trigonometric identities, and they have shown interpretable trends through the experiments. However, except for a few cases, we may not derive exact algorithms. The approximate solutions covering the entire modular operations remain as future works.

## Impact Statements

This paper presents work whose goal is to advance the field of Machine Learning. There are many potential societal consequences of our work, none which we feel must be specifically highlighted here.

## Acknowledgements

We thank Tadashi Kozuno for helpful discussion on this work. HF was supported by JSPS KAKENHI Grant Number JP22J21582.

## References

Akyürek, E., Schuurmans, D., Andreas, J., Ma, T., and Zhou, D. What learning algorithm is in-context learning? investigations with linear models. In *International Conference on Learning Representations*, 2023.

Barak, B., Edelman, B. L., Goel, S., Kakade, S. M., eran malach, and Zhang, C. Hidden progress in deep learning: SGD learns parities near the computational limit. In *Advances in Neural Information Processing Systems*, 2022.

Brown, T. B., Mann, B., Ryder, N., Subbiah, M., Kaplan, J., Dhariwal, P., Neelakantan, A., Shyam, P., Sastry, G., Askell, A., Agarwal, S., Herbert-Voss, A., Krueger, G., Henighan, T., Child, R., Ramesh, A., Ziegler, D. M., Wu, J., Winter, C., Hesse, C., Chen, M., Sigler, E., Litwin, M., Gray, S., Chess, B., Clark, J., Berner, C., McCandlish, S., Radford, A., Sutskever, I., and Amodei, D. Language models are few-shot learners. *arXiv preprint arXiv:2005.14165*, 2020.

Chughtai, B., Chan, L., and Nanda, N. A toy model of universality: Reverse engineering how networks learn group operations. *arXiv preprint arXiv:2302.03025*, 2023.

Conmy, A., Mavor-Parker, A. N., Lynch, A., Heimersheim, S., and Garriga-Alonso, A. Towards automated circuit discovery for mechanistic interpretability. In *Thirty-seventh Conference on Neural Information Processing Systems*, 2023.

Davies, X., Langosco, L., and Krueger, D. Unifying grokking and double descent. *arXiv preprint arXiv:2303.06173*, 2023.

Doshi, D., Das, A., He, T., and Gromov, A. To grok or not to grok: Disentangling generalization and memorization on corrupted algorithmic datasets. *arXiv preprint arXiv:2310.13061*, 2023.

Dziri, N., Lu, X., Sclar, M., Li, X. L., Jiang, L., Lin, B. Y., West, P., Bhagavatula, C., Bras, R. L., Hwang, J. D., Sanyal, S., Welleck, S., Ren, X., Ettinger, A., Harchaoui, Z., and Choi, Y. Faith and fate: Limits of transformers on compositionality. *arXiv preprint arXiv:2305.18654*, 2023.

Elhage, N., Nanda, N., Olsson, C., Henighan, T., Joseph, N., Mann, B., Askell, A., Bai, Y., Chen, A., Conerly, T., DasSarma, N., Drain, D., Ganguli, D., Hatfield-Dodds, Z., Hernandez, D., Jones, A., Kernion, J., Lovitt, L., Ndousse, K., Amodei, D., Brown, T., Clark, J., Kaplan, J., McCandlish, S., and Olah, C. A mathematical framework for transformer circuits. *Transformer Circuits Thread*, 2021. <https://transformer-circuits.pub/2021/framework/index.html>.

Elhage, N., Hume, T., Olsson, C., Schiefer, N., Henighan, T., Kravec, S., Hatfield-Dodds, Z., Lasenby, R., Drain, D., Chen, C., Grosse, R., McCandlish, S., Kaplan, J., Amodei, D., Wattenberg, M., and Olah, C. Toy models of superposition, 2022.

Furuta, H., Matsuo, Y., Faust, A., and Gur, I. Exposing limitations of language model agents in sequential-task compositions on the web. *arXiv preprint arXiv:2311.18751*, 2023.

Gromov, A. Grokking modular arithmetic. *arXiv preprint arXiv:2301.02679*, 2023.

Kumar, T., Bordelon, B., Gershman, S. J., and Pehlevan, C. Grokking as the transition from lazy to rich training dynamics. *arXiv preprint arXiv:2310.06110*, 2023.

Lee, N., Sreenivasan, K., Lee, J. D., Lee, K., and Papailiopoulos, D. Teaching arithmetic to small transformers. *arXiv preprint arXiv:2307.03381*, 2023.

Levi, N., Beck, A., and Bar-Sinai, Y. Grokking in linear estimators – a solvable model that groks without understanding. *arXiv preprint arXiv:2310.16441*, 2023.

Liu, Z., Kitouni, O., Nolte, N., Michaud, E. J., Tegmark, M., and Williams, M. Towards understanding grokking: An effective theory of representation learning. *arXiv preprint arXiv:2205.10343*, 2022.

Liu, Z., Michaud, E. J., and Tegmark, M. Omnidrok: Grokking beyond algorithmic data. In *International Conference on Learning Representations*, 2023a.

Liu, Z., Zhong, Z., and Tegmark, M. Grokking as compression: A nonlinear complexity perspective. *arXiv preprint arXiv:2310.05918*, 2023b.

Loshchilov, I. and Hutter, F. Decoupled weight decay regularization. In *International Conference on Learning Representations*, 2019.

Lyu, K., Jin, J., Li, Z., Du, S. S., Lee, J. D., and Hu, W. Dichotomy of early and late phase implicit biases can provably induce grokking. *arXiv preprint arXiv:2311.18817*, 2023.

Meng, K., Bau, D., Andonian, A., and Belinkov, Y. Locating and editing factual associations in gpt. *arXiv preprint arXiv:2202.05262*, 2023.

Merrill, W., Tsilivis, N., and Shukla, A. A tale of two circuits: Grokking as competition of sparse and dense subnetworks. *arXiv preprint arXiv:2303.11873*, 2023.

Miller, J., O'Neill, C., and Bui, T. Grokking beyond neural networks: An empirical exploration with model complexity. *arXiv preprint arXiv:2310.17247*, 2023.

Minegishi, G., Iwasawa, Y., and Matsuo, Y. Grokking tickets: Lottery tickets accelerate grokking. *arXiv preprint arXiv:2310.19470*, 2023.

Morwani, D., Edelman, B. L., Oncescu, C.-A., Zhao, R., and Kakade, S. Feature emergence via margin maximization: case studies in algebraic tasks. *arXiv preprint arXiv:2311.07568*, 2023.

Murty, S., Sharma, P., Andreas, J., and Manning, C. D. Grokking of hierarchical structure in vanilla transformers. *arXiv preprint arXiv:2305.18741*, 2023.

Nakkiran, P., Kaplun, G., Bansal, Y., Yang, T., Barak, B., and Sutskever, I. Deep double descent: Where bigger models and more data hurt. *arXiv preprint arXiv:1912.02292*, 2019.

Nanda, N., Chan, L., Lieberum, T., Smith, J., and Steinhardt, J. Progress measures for grokking via mechanistic interpretability. In *International Conference on Learning Representations*, 2023.

Notsawo, P. J. T., Zhou, H., Pezeshki, M., Rish, I., and Dumas, G. Predicting grokking long before it happens: A look into the loss landscape of models which grok. *arXiv preprint arXiv:2306.13253*, 2023.

Olah, C., Cammarata, N., Schubert, L., Goh, G., Petrov, M., and Carter, S. Zoom in: An introduction to circuits. *Distill*, 2020. doi: 10.23915/distill.00024.001. <https://distill.pub/2020/circuits/zoom-in>.

Olsson, C., Elhage, N., Nanda, N., Joseph, N., DasSarma, N., Henighan, T., Mann, B., Askell, A., Bai, Y., Chen, A., Conerly, T., Drain, D., Ganguli, D., Hatfield-Dodds, Z., Hernandez, D., Johnston, S., Jones, A., Kernion, J., Lovitt, L., Ndousse, K., Amodei, D., Brown, T., Clark, J., Kaplan, J., McCandlish, S., and Olah, C. In-context learning and induction heads. *Transformer Circuits Thread*, 2022. <https://transformer-circuits.pub/2022/in-context-learning-and-induction-heads/index.html>.

Power, A., Burda, Y., Edwards, H., Babuschkin, I., and Misra, V. Grokking: Generalization beyond overfitting on small algorithmic datasets. *arXiv preprint arXiv:2201.02177*, 2022.

Rubin, N., Seroussi, I., and Ringel, Z. Droplets of good representations: Grokking as a first order phase transition in two layer networks. *arXiv preprint arXiv:2310.03789*, 2023.

Stander, D., Yu, Q., Fan, H., and Biderman, S. Grokking group multiplication with cosets. *arXiv preprint arXiv:2312.06581*, 2023.

Tan, Z. and Huang, W. Understanding grokking through a robustness viewpoint. *arXiv preprint arXiv:2311.06597*, 2023.

Thilak, V., Littwin, E., Zhai, S., Saremi, O., Paiss, R., and Susskind, J. The slingshot mechanism: An empirical study of adaptive optimizers and the grokking phenomenon. *arXiv preprint arXiv:2206.04817*, 2022.

Varma, V., Shah, R., Kenton, Z., Kramár, J., and Kumar, R. Explaining grokking through circuit efficiency. *arXiv preprint arXiv:2309.02390*, 2023.

Vaswani, A., Shazeer, N., Parmar, N., Uszkoreit, J., Jones, L., Gomez, A. N., Kaiser, L., and Polosukhin, I. Attention is all you need. *arXiv preprint arXiv:1706.03762*, 2017.

Vig, J., Gehrmann, S., Belinkov, Y., Qian, S., Nevo, D., Singer, Y., and Shieber, S. Investigating gender bias in language models using causal mediation analysis. In Larochelle, H., Ranzato, M., Hadsell, R., Balcan, M., and Lin, H. (eds.), *Advances in Neural Information Processing Systems*, 2020.

Wei, J., Tay, Y., Bommasani, R., Raffel, C., Zoph, B., Borgeaud, S., Yogatama, D., Bosma, M., Zhou, D., Metzler, D., Chi, E. H., Hashimoto, T., Vinyals, O., Liang, P., Dean, J., and Fedus, W. Emergent abilities of large language models. *arXiv preprint arXiv:2206.08853*, 2022.

Xu, Z., Wang, Y., Frei, S., Vardi, G., and Hu, W. Benign overfitting and grokking in relu networks for xor cluster data. *arXiv preprint arXiv:2310.02541*, 2023.

Zhang, F. and Nanda, N. Towards best practices of activation patching in language models: Metrics and methods. *arXiv preprint arXiv:2309.16042*, 2024.

Zhong, Z., Liu, Z., Tegmark, M., and Andreas, J. The clock and the pizza: Two stories in mechanistic explanation of neural networks. In *Neural Information Processing Systems*, 2023.

Žunkovič, B. and Ilievski, E. Grokking phase transitions in learning local rules with gradient descent. *arXiv preprint arXiv:2210.15435*, 2022.

## Appendix

### A. Experimental Details

We summarize the hyper-parameters for the experiments (dimension in Transformers, optimizers, etc.) in Table 2. We provide the code in supplementary material.

Name	Value
Mod $p$	97
Epochs	1e6
Optimizer	AdamW (Loshchilov & Hutter, 2019)
Learning Rate	0.001
AdamW Betas	(0.9, 0.98)
Weight Decay $\lambda$	1.0
Batch Size	(Full batch)
Max Optimization Steps	3e5
Number of Seeds	3
Embedding Dimension $d_{\text{emb}}$	128
MLP Dimension $d_{\text{mlp}}$	512
Number of Heads	4
Head Dimension	32
Number of Layers	1
Activation	ReLU
Layer Normalization	False
Bias Term in Weight Matrix	False
Vocabulary Size $p'$	$p + n_{\text{op}}$ (including operation tokens)
Context Length	3

Table 2. Hyper-parameters for the grokking experiments. We follow the previous works (Power et al., 2022; Nanda et al., 2023; Zhong et al., 2023).

### B. Terminology for Mathematical Expressions

As a reference, we summarize the terminology for mathematical expressions in Table 3.

Term	Expressions
Modular Arithmetic	$(a \circ b) \% p = c$
Addition	$a + b$
Subtraction	$a - b$
Multiplication	$a * b$
Elementary Arithmetic	all the above (+, -, *)
Polynomials	$a^2 + b^2, a^3 + ab, (a + b)^4, \dots$ (including all the below)
Linear Expression (degree-1)	$2a - b, 2a + 3b, ab + b, \dots$
Cross Term	$ab, ab^2, \dots$
Quadratic Expression (degree-2)	$(a \pm b)^2, a^2 + ab, a^2 - b$
Cubic Expression (degree-3)	$(a \pm b)^3, \dots$
Quartic Expression (degree-4)	$(a \pm b)^4, \dots$
Factorizable Polynomials	$(a \pm b)^n, (a \pm b)^n \pm \sum (a \pm b)^k$ ( $n = 2, 3, \dots, k < n$ )
Polynomials with Cross Term	$a^2 + ab + b^2, a^3 + ab^2 + b, \dots$
(Non-Factorizable Polynomials)	
Sum of Powers	$a^n + b^n$ ( $n = 2, 3, \dots$ )

Table 3. Terminology for mathematical expressions in this paper.

## C. Mathematical Description of Transformer

In this section, we describe the structure of Transformer in our work, loosely following the notation of [Elhage et al. \(2021\)](#).

As defined in Section 3, we define embedding matrix as  $W_E$ , query, key, and value matrices of  $j$ -th head in the attention layer as  $W_Q^j, W_K^j, W_V^j$ . The input and output layer at the MLP block is denoted as  $W_{\text{in}}, W_{\text{out}}$ , and the unembedding matrix is denoted as  $W_U$ . We use ReLU for the activation functions and remove positional embedding, layer normalization, and bias terms for all the layers.

We also denote the token (one-hot representation of integers) in position  $i$  as  $t_i$ , the initial residual stream on  $i$ -th token as  $x_i^{(0)}$ , attention scores from the last tokens ( $t_2$ , because the context length is 3) to all previous tokens at  $j$ -th head as  $A^j$ , the attention output at  $j$ -th head as  $W_O^j$ , the residual stream after the attention layer on the final token as  $x^{(1)}$ , the neuron activations in the MLP block as “MLP”, and the final residual stream on the final token as  $x^{(2)}$ . “Logits” represents the logits on the final token since we only consider the loss from it.

We can formalize the logit calculation via the following equations.

- Embedding:  $x_i^{(0)} = W_E t_i$
- Attention score:  $A^j = \text{softmax}(x^{(0)T} W_K^j W_Q^j x_2^{(0)})$
- Attention block:  $x^{(1)} = x_2^{(0)} + \sum_j W_O^j W_V^j (x^{(0)} A^j)$
- MLP activations:  $\text{MLP} = \text{ReLU}(W_{\text{in}} x^{(1)})$
- MLP block:  $x^{(2)} = W_{\text{out}} \text{MLP} + x^{(1)}$
- Logits:  $W_U x^{(2)}$

Following the discussion in [Nanda et al. \(2023\)](#), we ignore the residual connection and investigate the neuron logit map  $W_L = W_U W_{\text{out}}$  as a dominant part to decide the logits.

## D. Proper Multi-Task Mixture also Accelerates Grokking in Polynomials

We also investigate the multi-task training with the mixture of polynomials; preparing the combination of operations as  $\{a + b, ab + b\}$ ,  $\{a^2 + b^2, a^2 + ab + b^2, (a + b)^2\}$ ,  $\{(a + b)^3, a^3 + ab\}$  and  $\{(a + b)^3, a^3 + ab^2 + b\}$ .

As shown in [Figure 11](#) and [Figure 12](#), a proper mixture of polynomials, in terms of operation similarity, also accelerates grokking in multi-task settings. For instance,  $a^2 + b^2$  and  $(a + b)^2$  help generalization in  $a^2 + ab + b^2$ . This implies that the required representations among  $\{a^2 + b^2, a^2 + ab + b^2, (a + b)^2\}$  would be the same while original single-task  $a^2 + ab + b^2$  fails to grok due to the low signal-to-noise ratio from the non-factorizable cross term. The test accuracy also improves in the cubic expression ([Figure 12](#)). However, it hits a plateau before the perfect generalization.

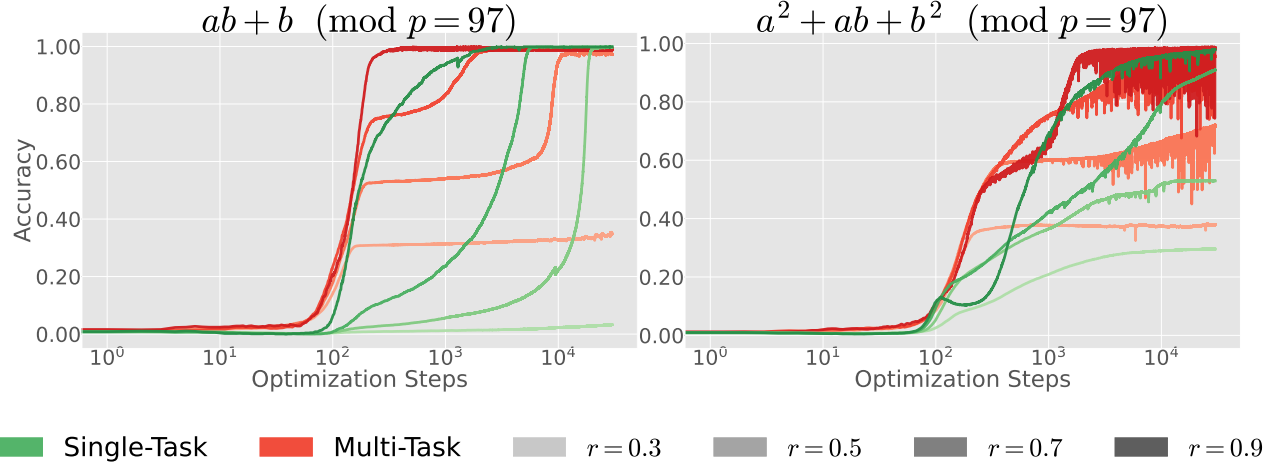


*Figure 11.* Test accuracy in grokking with a mixture of modular polynomials ( $\{a + b, ab + b\}$  and  $\{a^2 + b^2, a^2 + ab + b^2, (a + b)^2\}$ ). The multi-task training across similar operations promotes grokking.

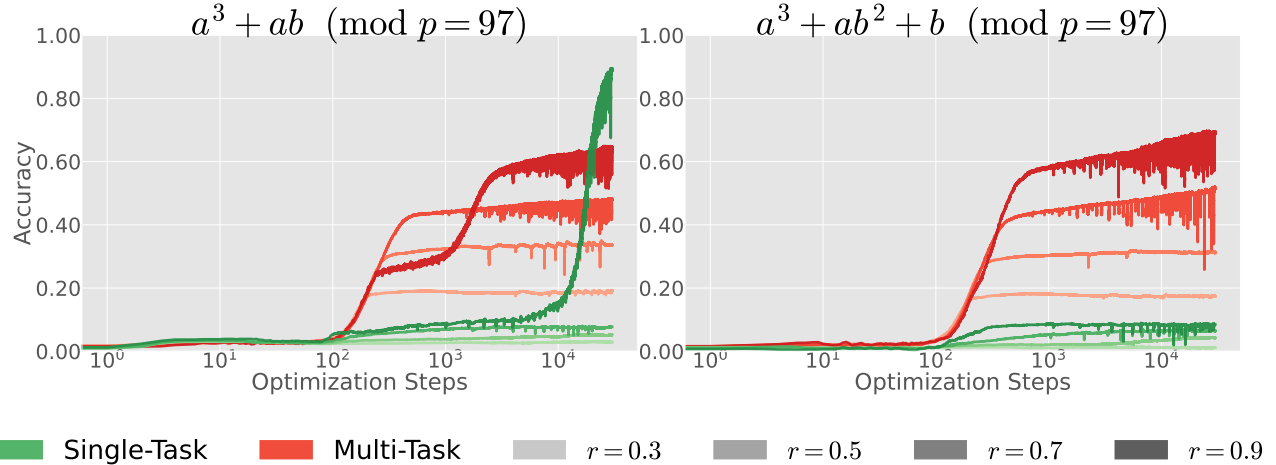


*Figure 12.* Test accuracy in grokking with a mixture of modular polynomials ( $\{(a + b)^3, a^3 + ab\}$  and  $\{(a + b)^3, a^3 + ab^2 + b\}$ ). The multi-task training across similar operations promotes the improvement of test accuracy.

## E. Analysis of Restricted Loss in Modular Subtraction

In Figure 13, we test the restricted loss and ablated loss, the metrics proposed by Nanda et al. (2023), where the restricted loss is calculated only with the Fourier components of key frequencies, and the ablated loss is calculated by removing a certain frequency from the logits. The results show that modular subtraction has several *dependent* frequencies, which cause worse restricted loss if ablated, while they are not key frequencies (we set the threshold to  $\Delta\mathcal{L} > 1e-9$ ). Those dependent frequencies are not observed in modular addition. Moreover, the restricted loss for modular subtraction significantly gets worse than the original loss, which also emphasizes the subtle dependency on other frequency components.

Moreover, we extensively evaluate the relationships between loss and Fourier components. We here decompose the logits as follows:

$$\text{Logits} = (\text{Logits from key frequencies}) + (\text{Logits from non-key frequencies}) + (\text{Logits from residuals}),$$

where logits from residuals are estimated by subtracting logits of all the frequencies from the raw logits.

The results are presented in Table 4. In modular addition, we find that key frequencies contribute to the prediction and non-key frequencies only have a negligible effect on the loss (e.g. train loss v.s. ablation (d), restricted loss v.s. ablation (c)). The residuals actually hinder prediction accuracy (e.g., train loss v.s. ablation (c)). In modular subtraction, any ablations drop the performance and all the components contribute to the predictions, which implies that the grokked models in modular subtraction have informative representations to some degree over all the frequencies, even residuals in the logits.

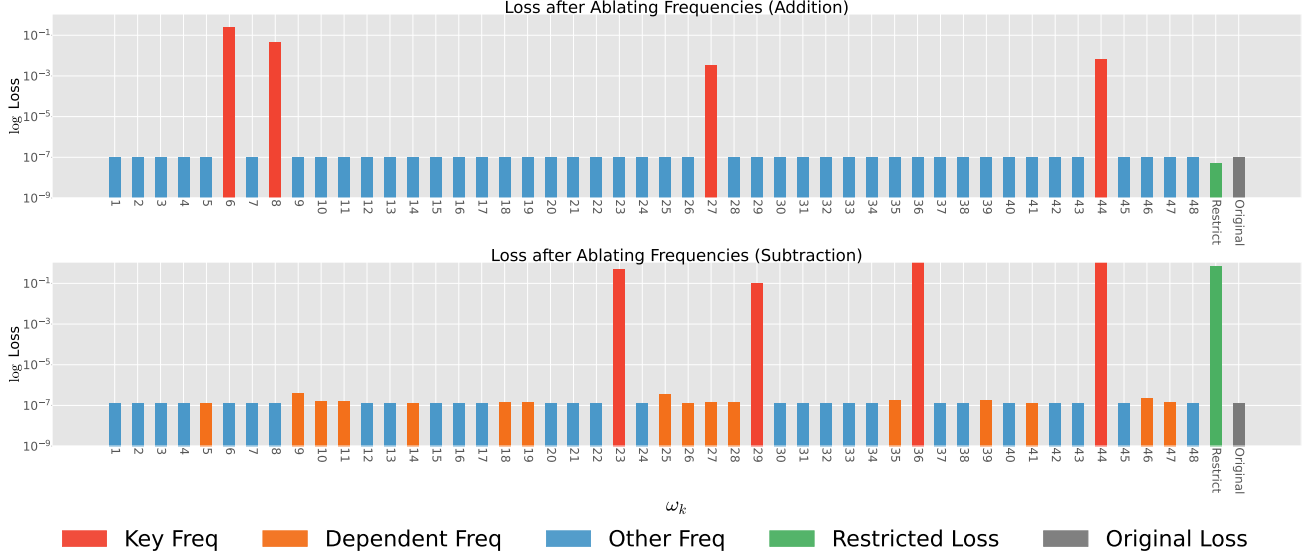


Figure 13. Loss of Transformer when ablating each frequency ( $k = 1, \dots, 48$ ) and everything except for the key frequencies (restricted loss). In modular subtraction, we find several *dependent* frequencies (orange), which cause worse restricted loss if ablated while they are not key frequencies.

	Logits			Loss ( $\downarrow$ )	
	Key Freq.	Non-key Freq.	Residuals	Add (+)	Sub (-)
Train Loss	✓	✓	✓	1.008e-7	1.336e-7
Restricted Loss	✓			4.985e-8	7.141e-1
Ablation (a)		✓		4.576	7.741
(b)			✓	5.385	2.179e+1
(c)	✓	✓		4.989e-8	5.582e-1
(d)	✓		✓	1.015e-7	5.348e-6
(e)		✓	✓	5.383	2.188e+1

Table 4. Loss of Transformer when ablating the components of key frequencies, non-key frequencies, and residuals, from the logits.

## F. Grokking with Frozen Random Embedding

We here show that even if the sparsity and non-trivial biases are not realizable in embedding, grokking could occur in Figure 14. In this experiment, we initialize embedding weights from Gaussian distribution and then freeze them not allowing any parameter updates during training. Even with the restricted capacity, the models exhibit grokking in elementary arithmetic.

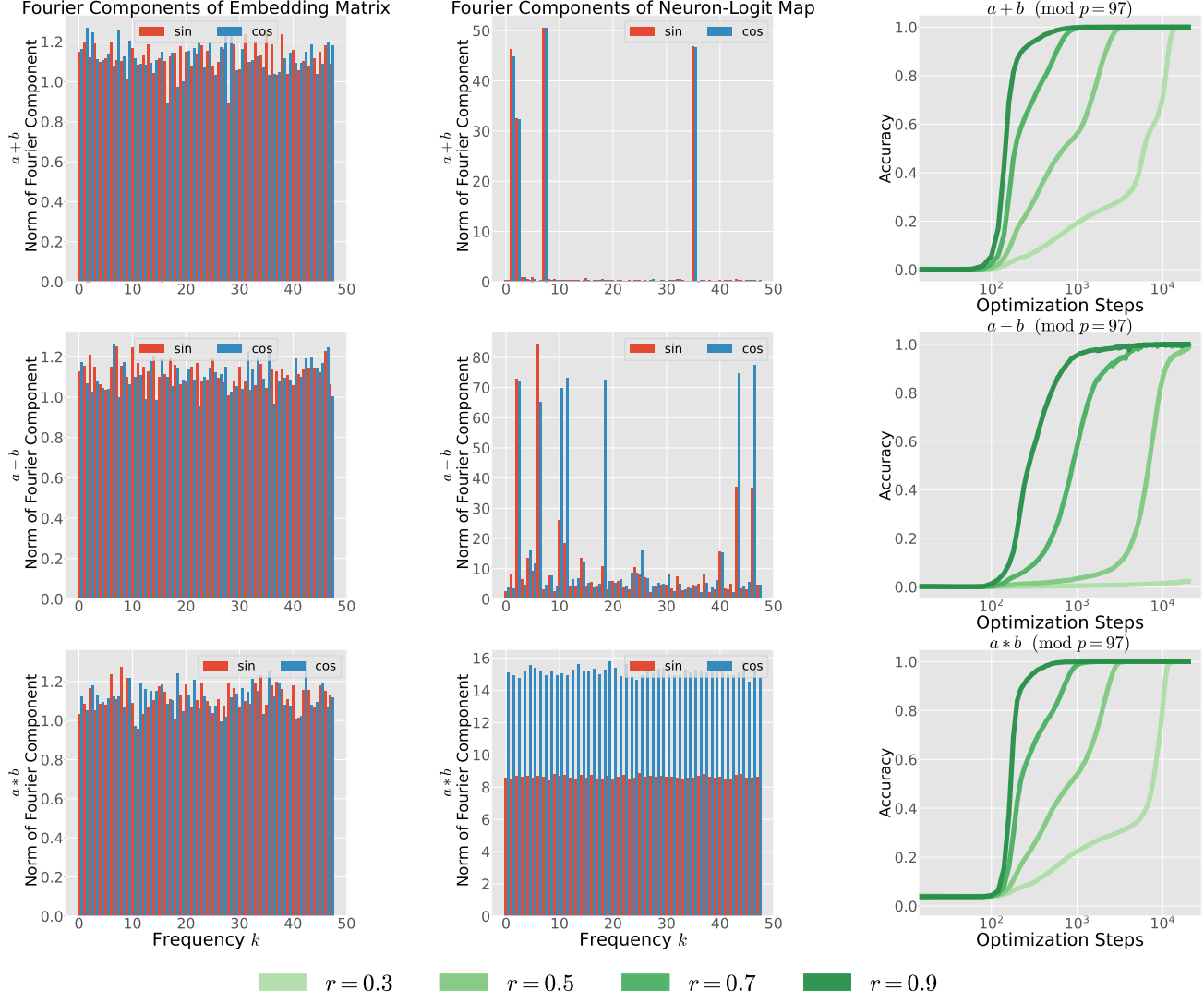


Figure 14. Test accuracy with elementary arithmetic from random embedding. Grokking can occur even using frozen random embedding, while unembedding obtains similar Fourier representation as discussed in Section 5.

## G. Enlarged Figures

In this section, we provide the enlarged figures from the main text for visibility. Those have the same contents as the original figures.

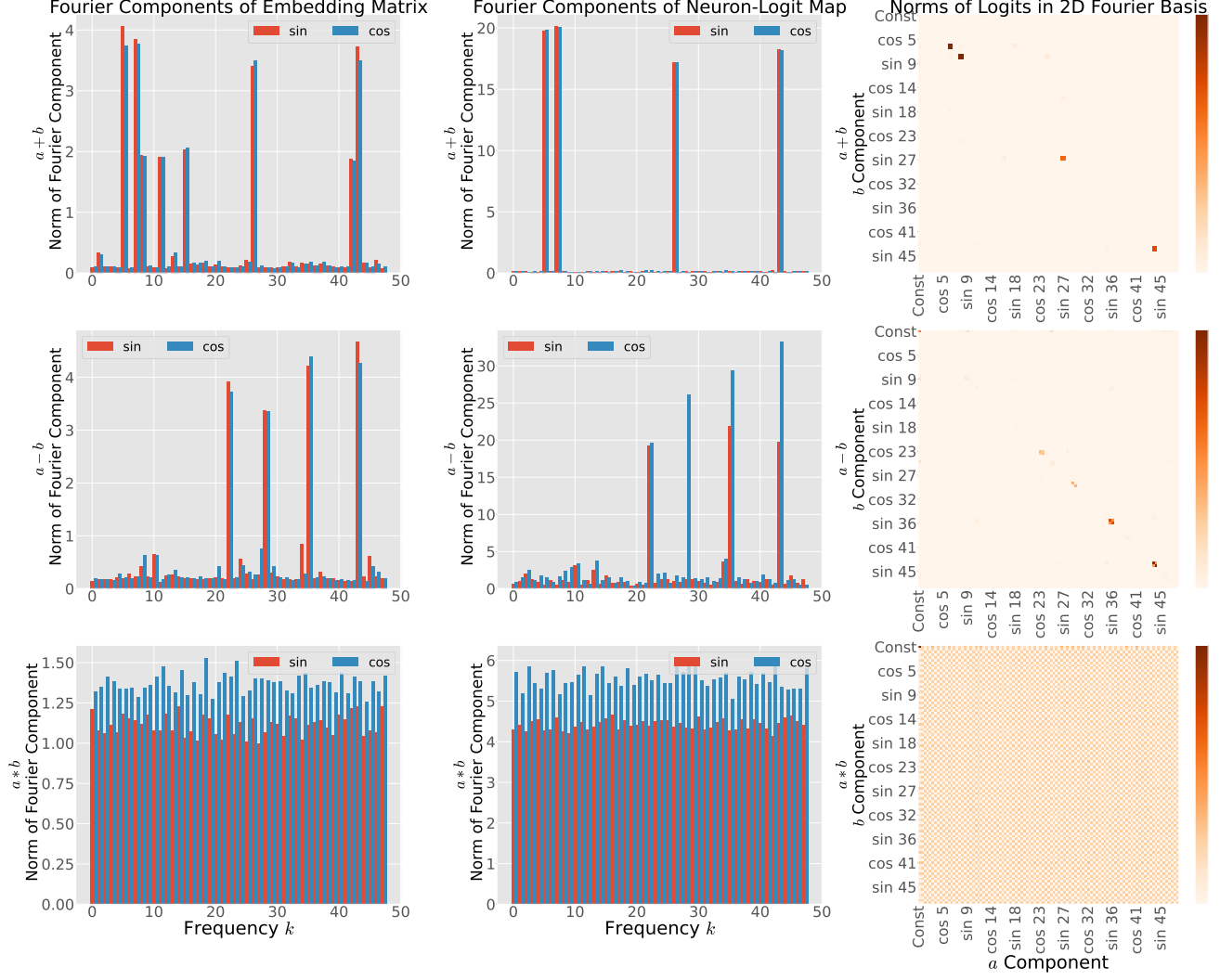


Figure 15. Frequency analysis in grokking with elementary arithmetic (the same as Figure 3).

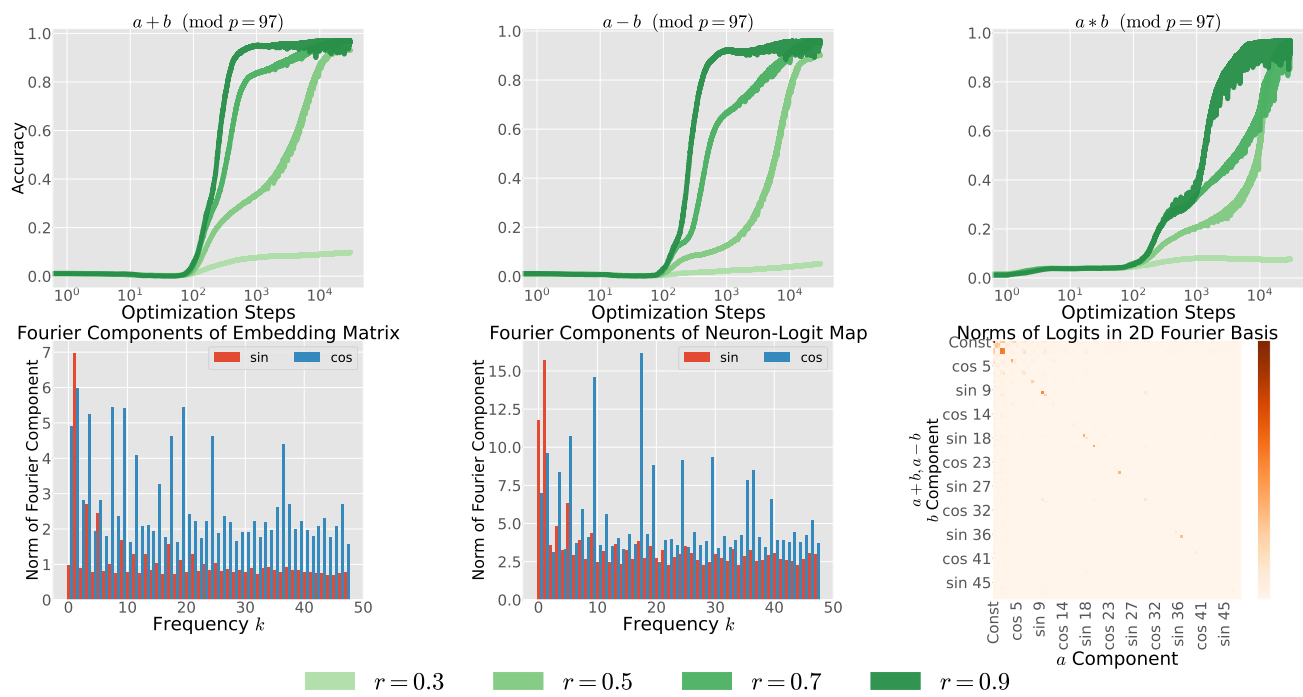


Figure 16. Test accuracy (above) and frequency analysis (below) in a mixture of modular elementary arithmetic (the same as Figure 4).

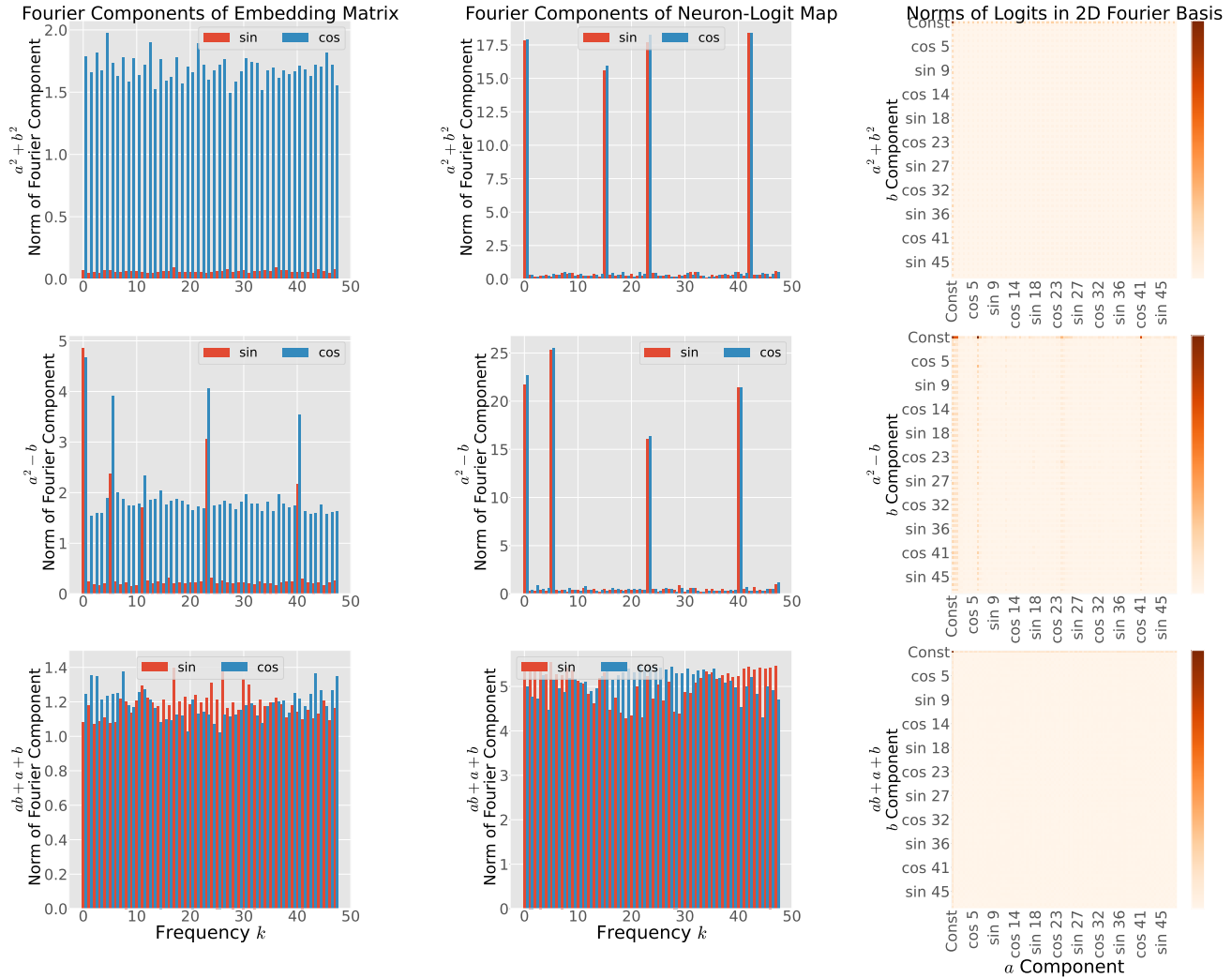


Figure 17. Frequency analysis in grokking with modular polynomials (the same as Figure 6).

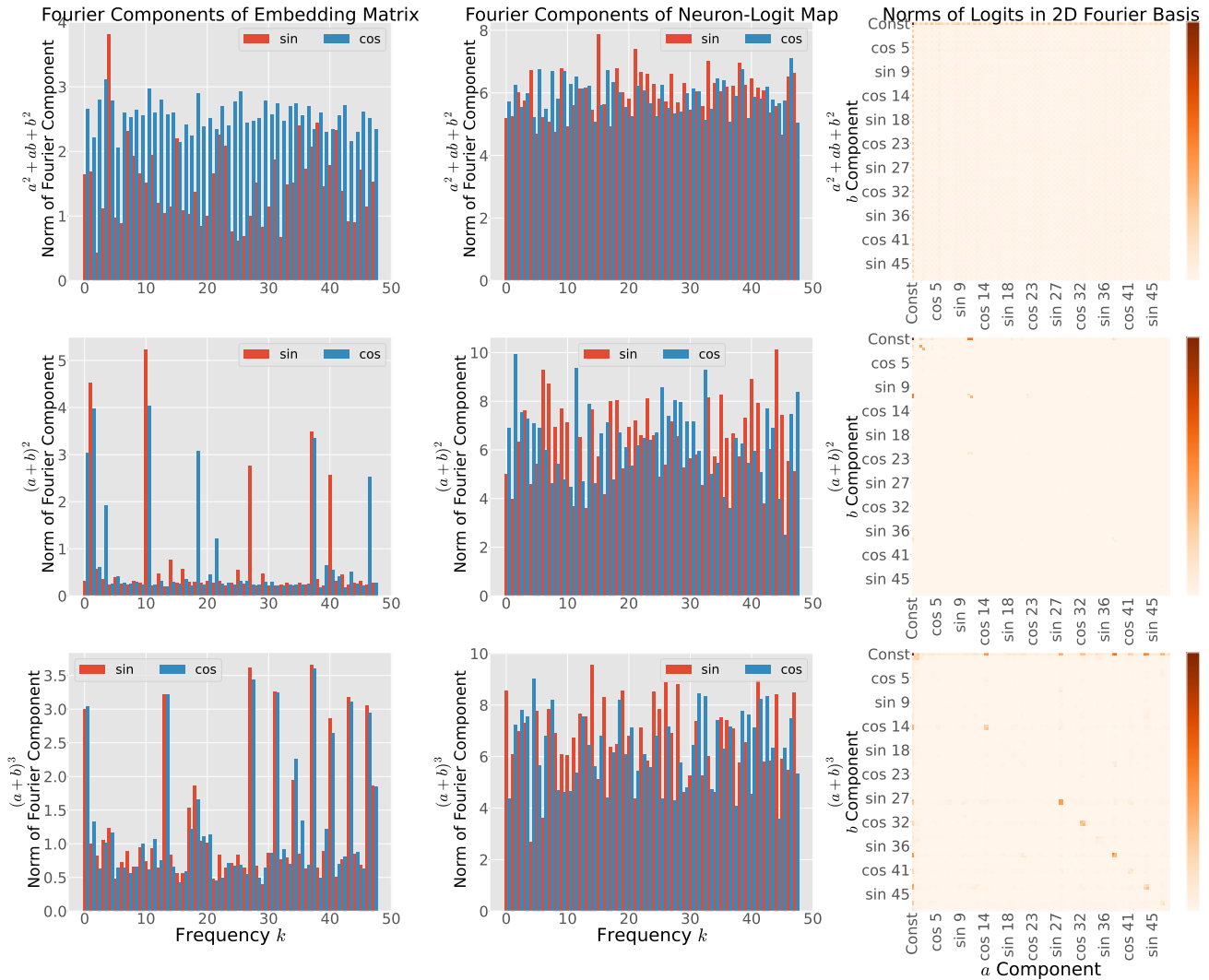


Figure 18. Frequency analysis in grokking with factorizable modular polynomials (the same as Figure 8).

## H. FFS and FCR in Neuron-Logit Map

Figure 19 presents our progress measures: FFS and FCR in neuron-logit map  $W_L$ . For elementary arithmetic operators, the dynamics seem to be the same as seen in embedding (Figure 10). This might be due to the similarity of embedding and neuron-logit map (Figure 3). For sum of powers ( $a^n + b^n$ ) and the factorizable ( $((a + b)^n)$  behaves differently from embedding (Figure 10). The sum of powers decreases FFS while keeping FCR relatively higher. The factorizable polynomials maintain both FFS and FCR relatively higher. This might be due to the representation asymmetry between embedding and neuron-logit map in polynomials (Figure 8).

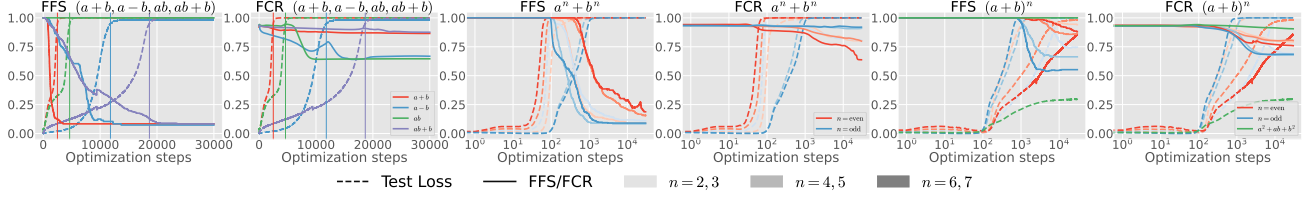


Figure 19. FFS and FCR in neuron-logit map for each operation  $(a + b, a - b, a * b, ab + b, a^n + b^n, (a + b)^n)$ .

## I. Summary of Grokked Modular Operators

Table 5 summarizes if each modular operator can cause grokking in  $r = 0.3$  or not. We provide the best test accuracy if they do not grok.

Fraction	Elementary Arithmetic			Linear Expression								
	$a + b$	$a - b$	$a * b$	$2a + b$	$a + b \rightarrow 2a + b$	$2a - b$	$a + b \rightarrow 2a - b$	$2a + 3b$	$a + b \rightarrow 2a + 3b$	$2a - 3b$	$a + b \rightarrow 2a - 3b$	
$r = 0.3$	✓		✓		3.1%		✓		2.5%		✓	3.7%
$r = 0.4$	✓		✓		9.0%		✓		✓		✓	✓
$r = 0.5$	✓		✓			✓		✓		✓		✓
$r = 0.6$	✓		✓			✓		✓		✓		✓
$r = 0.7$	✓		✓			✓		✓		✓		✓
$r = 0.8$	✓		✓			✓		✓		✓		✓
$r = 0.9$	✓		✓			✓		✓		✓		✓
Cross Term (Degree-1)												
Fraction	$ab + a + b$	$ab + b$	$a * b \rightarrow ab + b$	$ab - b$	$a * b \rightarrow ab - b$	$a^2 + b$	$a^2 - b$	$a^3 + 2b$	$a^3 - 2b$			
	✓		6.1%	✓		✓		9.5%		✓		✓
$r = 0.3$	✓		9.7%	✓		✓				✓		✓
$r = 0.4$	✓			✓		✓		✓		✓		✓
$r = 0.5$	✓			✓		✓		✓		✓		✓
$r = 0.6$	✓			✓		✓		✓		✓		✓
$r = 0.7$	✓			✓		✓		✓		✓		✓
$r = 0.8$	✓			✓		✓		✓		✓		✓
$r = 0.9$	✓			✓		✓		✓		✓		✓
Cross Term (Degree-n)												
Fraction	$a^2 + ab + b^2$	$a^2 + ab + b^2 + a$	$a^3 + ab$	$a^3 + ab^2 + b$	$a^2 + b^2$	$a^2 - b^2$	$a^3 + b^3$	$a^4 + b^4$	$a^5 + b^5$	$a^6 + b^6$	$a^7 + b^7$	
	34%	4.8%	4.9%	4.0%	✓	✓	✓	✓	✓	✓	✓	
$r = 0.3$	47%	8.2%	9.4%	7.8%	✓	✓	✓	✓	✓	✓	✓	
$r = 0.4$	56%	10%	11%	10%	✓	✓	✓	✓	✓	✓	✓	
$r = 0.5$	65%	13%	13%	12%	✓	✓	✓	✓	✓	✓	✓	
$r = 0.6$	74%	17%	14%	13%	✓	✓	✓	✓	✓	✓	✓	
$r = 0.7$					✓	✓	✓	✓	✓	✓	✓	
$r = 0.8$	✓	42%	16%	15%	✓	✓	✓	✓	✓	✓	✓	
$r = 0.9$	✓	67%	✓	18%	✓	✓	✓	✓	✓	✓	✓	
Factorizable												
Fraction	$(a + b)^2$	$(a + b)^2 + a + b$	$a^2 - b^2$	$(a - b)^2$	$(a + b)^3$	$(a - b)^3$	$(a + b)^4$	$(a - b)^4$	$(a + b)^5$	$(a + b)^6$	$(a + b)^7$	
	✓		✓	✓	✓		5.9%	✓	85%	✓	✓	
$r = 0.3$	✓		✓	✓	✓		12%	✓	91%	✓	✓	
$r = 0.4$	✓		✓	✓	✓			✓	91%	✓	✓	
$r = 0.5$	✓		✓	✓	✓			✓	92%	✓	✓	
$r = 0.6$	✓		✓	✓	✓			✓		✓	✓	
$r = 0.7$	✓		✓	✓	✓			✓		✓	✓	
$r = 0.8$	✓		✓	✓	✓			✓		✓	✓	
$r = 0.9$	✓		✓	✓	✓			✓		✓	✓	

Table 5. Summary of grokked modular operators tested in this paper ( $p = 97$ ). We provide the best test accuracy if the operator does not cause grokking.

### J. Grokking Can be a Function of Modulo $p$

In addition to mathematical operation and dataset fraction, grokking can be a function of modulo  $p$ . Figure 20 shows that  $p = 97$  causes grokking with  $a^3 + ab$ , while  $p = 59$  and  $p = 113$  do not. Surprisingly,  $p = 59$  has fewer combinations than  $p = 97$ , but  $p = 59$  does not generalize to the test set even with  $r = 0.9$ . The results suggest that we might need to care about the choice of  $p$  for grokking analysis.

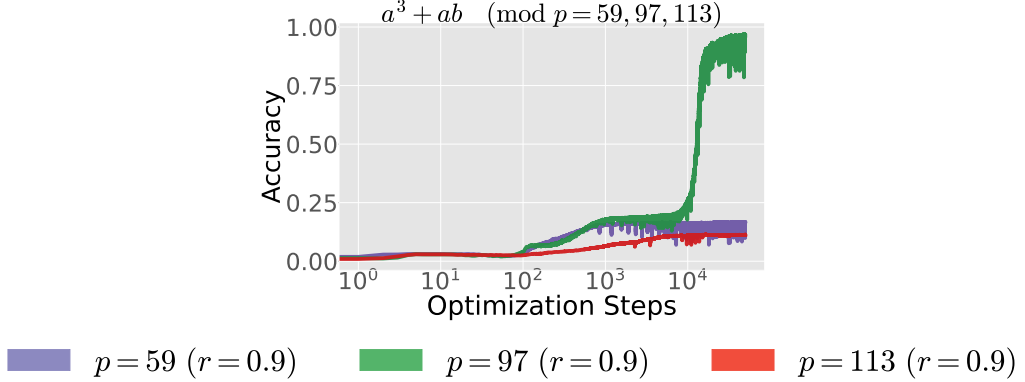


Figure 20. Test accuracy in grokking with  $a^3 + ab$  ( $r = 0.9$ ).  $p = 97$  only causes grokking among 59, 97, 113.

### K. Dataset Distribution Does not Have Significant Effects

One possible hypothesis why some modular polynomials are hard to generalize is that some polynomials bias the label distribution in the dataset. To examine this hypothesis, we calculate several statistics on label distribution in the dataset. We first randomly split train and test dataset ( $r = 0.3$ ), and get categorical label distributions. We compute the KL divergence between train label distribution  $d_{\text{train}}$  and test label distribution  $d_{\text{test}}$ , train label entropy, and test label entropy, averaging them with 100 random seeds.

Figure 21 shows KL divergence between train and test datasets (top), train dataset entropy (middle), and test dataset entropy (bottom). While those values slightly differ across the operations, there are no significant difference between generalizable (e.g.  $a^3 + b^3$ ,  $a^2 + b^2$ ) and non-generalizable (e.g.  $a^3 + ab$ ,  $a^2 + ab + b^2$ ) polynomials despite their similarity. The results do not imply that dataset distribution has significant impacts on grokking.

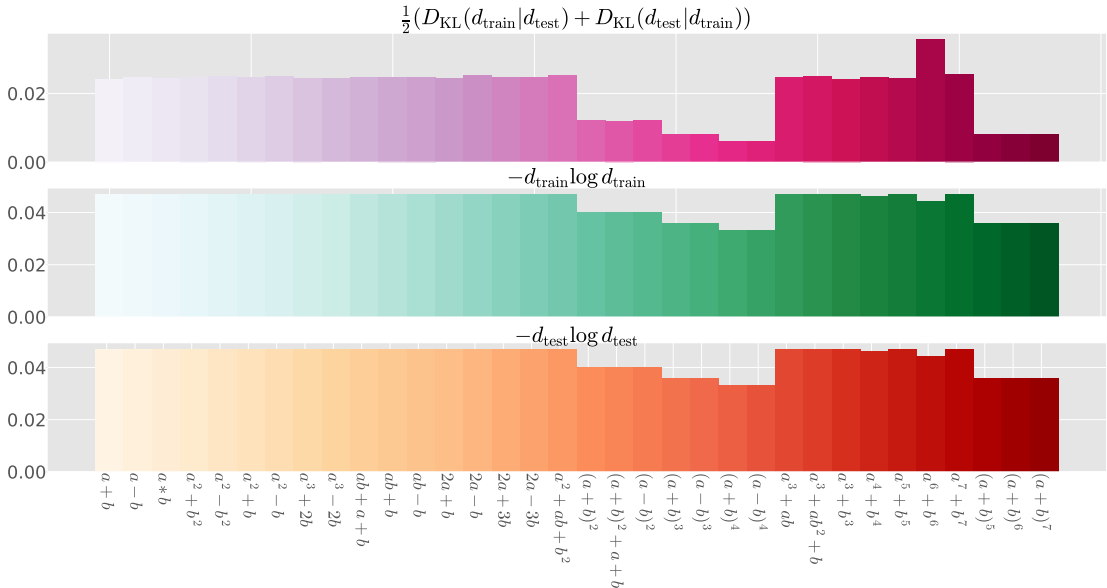


Figure 21. KL divergence between train and test datasets (top), train dataset entropy (middle), and test dataset entropy (bottom).

## L. Pre-Grokked Models May not Help Higher-Order Polynomials

In Section 6.3, we demonstrate that pre-grokked models accelerate grokking in linear expressions. We here extensively test pre-grokked models in higher-order polynomials (quadratic and cubic). The results are shown in Table 6, which implies that pre-grokked models may not help grokking accelerations. This also suggests that while the learned representation of polynomials seems to be a superposition of that of elementary arithmetic (e.g. Section 6.1), their functionalities might differ significantly.

Downstream Op.	Addition ( $a + b$ )		Multiplication ( $a * b$ )		Subtraction ( $a - b$ )		From Scratch
	PT-E	PT-T	PT-E	PT-T	PT-E	PT-T	
$2a + b$	✓	✓	✗	✓	$r = 0.4$	✓	$r = 0.5$
$2a - b$	✓	✓	✗	✓	✓	$r = 0.5$	$r = 0.4$
$2a + 3b$	✓	✓	✗	✓	$r = 0.4$	✗	$r = 0.4$
$2a - 3b$	✓	✓	✗	✓	$r = 0.4$	✓	$r = 0.4$
$ab + b$	✗	✓	$r = 0.4$	✓	✗	✓	$r = 0.5$
$ab - b$	✗	$r = 0.4$	$r = 0.4$	✓	✗	✓	$r = 0.5$
$(a + b)^2$	✓	✓	$r = 0.8$	✓	✓	$r = 0.9$	✓
$(a - b)^2$	✓	✗	$r = 0.9$	✗	✓	$r = 0.8$	✓
$(a + b)^2 + a + b$	✓	$r = 0.4$	✗	✓	✓	✓	✓
$a^2 + ab + b^2$	$r = 0.9$	✗	$r = 0.7$	✗	$r = 0.9$	✗	$r = 0.8$
$a^2 - b$	$r = 0.4$	✓	✗	✓	$r = 0.6$	✓	$r = 0.4$
$a^2 - b^2$	$r = 0.6$	$r = 0.7$	$r = 0.6$	$r = 0.5$	$r = 0.7$	$r = 0.4$	✓
$(a + b)^3$	✓	✗	✗	✗	$r = 0.6$	✗	✓
$(a - b)^3$	$r = 0.4$	✗	✗	✗	$r = 0.6$	✗	$r = 0.5$
$a^3 + ab$	✗	✗	✗	✗	✗	✗	$r = 0.9$
$a^3 + ab^2 + b$	✗	✗	✗	✗	✗	✗	✗

Table 6. Summary of grokked modular operators with pre-grokked models (both embedding and Transformer). We provide the smallest train fraction where grokking happens. PG-E/T stands for pre-grokked embedding/Transformer. The shaded ones are the results presented in Figure 9.

## M. Extended Limitation

Our work extends the grokking analysis from simple modular addition to complex modular polynomials. However, those tasks are still synthetic and far from LLMs (Brown et al., 2020), the most popular application of Transformers. Connecting grokking phenomena or mechanistic interpretability analysis into the emergent capability (Wei et al., 2022), or limitation in compositional generalization (Dziri et al., 2023; Furuta et al., 2023) and arithmetic (Lee et al., 2023) would be interesting future directions.